Advances in Engineering Research, volume 146

4th International Conference on Material Engineering and Application (ICMEA 2017)

$Ca_{0.5}Mg_{0.5}Co_2O_4$ Nanosheets Comprised of Nanoparticles, Synthesis, Characterization and their Catalytic Activity in the Hydrolysis of Ammonia Borane for Hydrogen Production

Liling LI[a]
Department of pharmacy
Huizhou Health Sciences Polytechnic
Huizhou, China

Xiuxia FENG[b], Jinyun LIAO[b*], Guiqiang DIAO[b], Xibin ZHANG[b], Hao LI[b]
School of chemistry and Materials Engineering
Huizhou University
Huizhou, China
e-mail: jyliao@126.com

***Abstract*—Catalytic hydrolytic reaction of ammonia borane (AB) is regarded as safe and efficient way to produce hydrogen. However, the development of heterogeneous catalysts with both high catalytic performance and low cost for this hydrolytic reaction is still a great challenge. In this work, we have developed a novel catalyst for the hydrolysis of ammonia borane, $Ca_{0.5}Mg_{0.5}Co_2O_4$ nanosheets composed of nanoparticles, which was characterized by X-ray powder diffractometer, field emission scanning electron microscope, transmission electron microscope, and volumetric analyzer. In the AB hydrolysis, the hydrogen production rate will increase as the increase the NaOH dosage. At NaOH dosage of 1.6 g, the turnover frequency is 4.8 $mol_{hydrogen}$ min^{-1} mol_{cat}^{-1}. It is also found that a high catalyst dosage and a high reaction temperature are favorable for the fast hydrogen release from AB solution.**

Keywords-hydrogen production; ammonia borane; nanosheets; catalysis

I. INTRODUCTION

The excessive consumption of fossil fuels in the word causes serious environmental pollution and greenhouse effect. It is inevitable for our human being to cut down the usage of fossil fuels and replace these nonrenewable resources with other clean, renewable energy. Hydrogen is regarded as an ideal energy carrier, which has several advantages including its high energy density, together with the environmental benign nature [1, 2]. Recently, different methods have been developed and implemented to produce hydrogen [3-7]. Among them, the production of hydrogen by the catalytic dehydrogenation of ammonia borane (AB, NH_3BH_3) in aqueous solution has received special attention because AB is an excellent hydrogen-storage material with a high gravimetric hydrogen content of up to 19.6 wt% (nearly 5 times higher than that of traditional metal hydride materials). This value is several times higher than the target for the year of 2020 set by the U.S. Department of Energy (currently set at 5.5 wt% H_2) [8]. At room temperature, AB is very stable in aqueous solution. However, the hydrolysis of AB only occurs and hydrogen can be continuously produced in the presence of a proper catalyst. The heterogeneous catalysts towards the AB hydrolysis can be classed into two groups. The first group is the noble metal or alloy catalyst, such as Pt [9, 10], Ru [11, 12] and PdPt [13]. It has been well demonstrated that these catalysts exhibit high activity towards the AB hydrolysis. However, the high cost of these catalysts hinders their industrial applications. Although their cost can be slightly reduced by alloying the noble metal with cheaper metals, such as Cu and Co [14, 15], the resulted alloy catalysts is still not cost-effective. The second group is the noble-metal-free catalysts, such as Co [16], Ni [17] and their alloys [18, 19]. Generally speaking, this group of catalysts shows relatively low catalytic activity and poor stability in contrast to noble metal catalysts, which cannot meet the requirement for practical applications. In this sense, the development of other types of catalyst for the AB hydrolysis is highly desirable.

In this work, we have prepared $Ca_{0.5}Mg_{0.5}Co_2O_4$ nanosheets composed of nanoparticles. Their catalytic activities towards the AB hydrolysis were investigated. As far as we know, $Ca_{0.5}Mg_{0.5}Co_2O_4$ as a catalyst for the AB hydrolysis has not yet been reported in the literature. It is found that the TOF for the as-prepared $Ca_{0.5}Mg_{0.5}Co_2O_4$ nanosheets in the dehydrogenation of AB can reach about 4.8 $mol_{hydrogen}$ min^{-1} mol_{cat}^{-1}, which exhibits higher activity than many noble-metal-free catalysts in the documents.

II. EXPERIMENTAL

A. Synthesis

Ultrapure water was used all throughout the experiments. All reagents were of nalytic Grade (AR). For the synthesis of $Ca_{0.5}Mg_{0.5}Co_2O_4$ nanosheets, 4.0 mmol $CoCl_2$, 1.0 mmol $MgCl_2$ and 1.0 mmol $CaCl_2$ were mixed in 20 mL water under stirring. 24 mmol urea was dissolved in 40 mL water. After these two solutions were mixed, the resultant transparent solution was poured in a Teflon-lined stainless

autoclave, which was sealed and then place into a drying oven at 160 ℃ for 8 h. The resulted power in the bottom of autoclave was collected and calcined at 500 ℃ for 5 h.

B. Characterization

The phase and purity of the samples were analyzed by using a X-ray powder Diffractometer (XRD) (TTR3, Regaku, Japan) with a Cu Kαradiation (λ = 1.5406A). The morphology of the samples was observed by a field emission scanning electron microscope (SU8010, Hitachi, Japan). Specific surface area was measured by Brunauer-Emmett-Teller (BET) method based on the sorption isotherms obtained on a Quantachrome Autosorb-1 volumetric analyzer.

C. Catalytic experiments

The catalytic activity of our catalysts in the hydrolytic dehydrogenation of AB was determined by measuring the rate of hydrogen generation. If not specified, the catalytic experiments were performed at 308 K. Typically, 10.0 mg catalyst was added in a glass reaction vessel, which was placed into a water bath for maintaining the reaction temperature. Then, 20 mL of mixed solution containing AB (2.8 mmol) and NaOH (20 mmol) was added into the vessel. As soon as the catalyst came into contact with AB solution, many bubbles were generated. The volume of generated gas during the hydrolysis reaction was monitored using the gas burette by water displacement.

III. RESULTS AND DISCUSSION

The obtained $Ca_{0.5}Mg_{0.5}Co_2O_4$ nanosheets were characterized with XRD and the result is shown in Figure 1. Cleary, Seven peaks at 2θ = 29.8 °, 31.2 °, 36.9 °, 38.4 °, 44.7 °, 59.3 ° and 65.54 ° are observed, which corresponds to the cubic phase of $CaCo_2O_4$ (JCPDS 51-0311) or $MgCo_2O_4$ (JCPDS 02-1073). In our synthetic process, Ca^{2+}, Mg^{2+} and Co^{2+} will react with basic and the mixed hydroxides are produced. When these mixture are heated, they will lose water to form the oxides. At the same time, Co(I) will be oxidized to Co(III) at high temperature. The $Ca_{0.5}Mg_{0.5}Co_2O_4$ sample is formed via the following reactions:

$$Ca^{2+} + OH^- \rightarrow Ca(OH)_2 \quad (1)$$

$$Mg^{2+} + OH^- \rightarrow Mg(OH)_2 \quad (2)$$

$$Co^{2+} + OH^- \rightarrow Co(OH)_2 \quad (3)$$

$$0.5Ca(OH)_2 + 0.5Mg(OH)_2 + 2Co(OH)_2 + 0.5O_2 \rightarrow Ca_{0.5}Mg_{0.5}Co_2O_4 + 3H_2 \quad (4)$$

The morphology of the $Ca_{0.5}Mg_{0.5}Co_2O_4$ sample is investigated with SEM and the results are shown in Figure 2. Figure 2a is the low-magnification SEM images of the $Ca_{0.5}Mg_{0.5}Co_2O_4$ sample, demonstrating the numerous nanosheets can be obtained by our synthetic approach. Figure 2b indicates that the typical size of these nanosheets is 1-2 μm. Figure 2c reveals that the nanosheets are composed of nanoparticles. Figure 2d is the cross-section SEM image of the $Ca_{0.5}Mg_{0.5}Co_2O_4$nanosheets, indicating the thickness of the nanosheets is around 50 nm. The TEM analysis on a selected $Ca_{0.5}Mg_{0.5}Co_2O_4$ nanosheet is carried out and results are shown in Figure 2e and 2f. Figure 2e is the low-magnification TEM images of the $Ca_{0.5}Mg_{0.5}Co_2O_4$ sample, confirming the nanosheet structure of the obtained product. Figure 2f further demonstrated that the nanosheet is composed of nanoparticles.

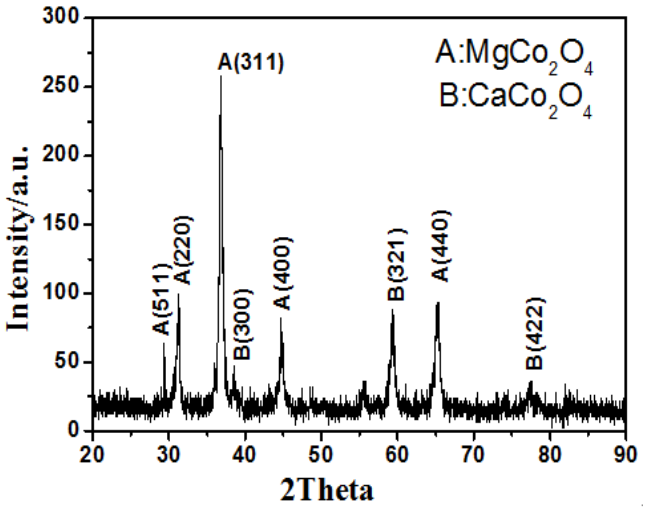

Figure 1. XRD pattern of $Ca_{0.5}Mg_{0.5}Co_2O_4$ sample.

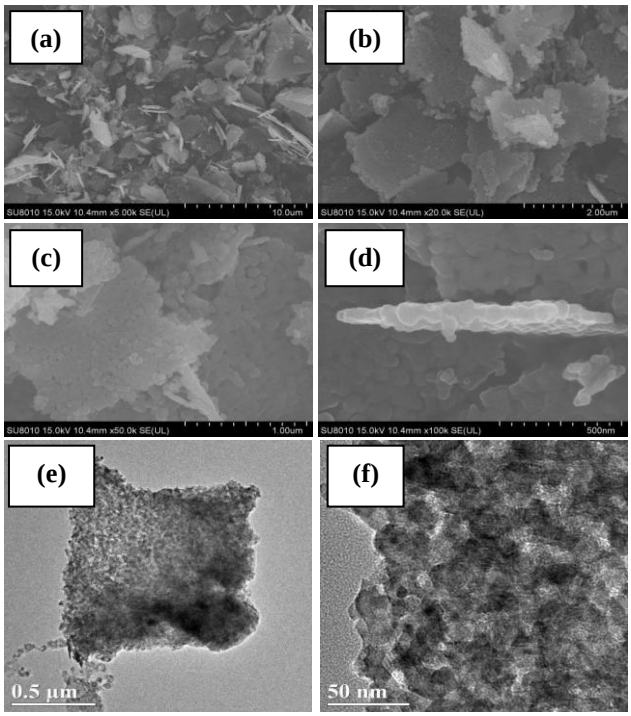

Figure 2. SEM images (a-d) and TEM images (e-f) of Ca0.5Mg0.5Co2O4 sample.

The $Ca_{0.5}Mg_{0.5}Co_2O_4$ nanosheets were characterized by adsorption-desorption isotherms of N_2 (Figure 3). As displayed, the isotherms can be classified as type IV isotherm in the classification of IUPAC. $Ca_{0.5}Mg_{0.5}Co_2O_4$ nanosheets show adsorption-desorption hysteresis at relative pressure range of 0.45~0.98, demonstrating the existence of the mesopores. It is possible that these mesopores are derived from the gap of different nanoparticles, as shown in Figure 2f. The BET surface area is about 27 $m^2 g^{-1}$.

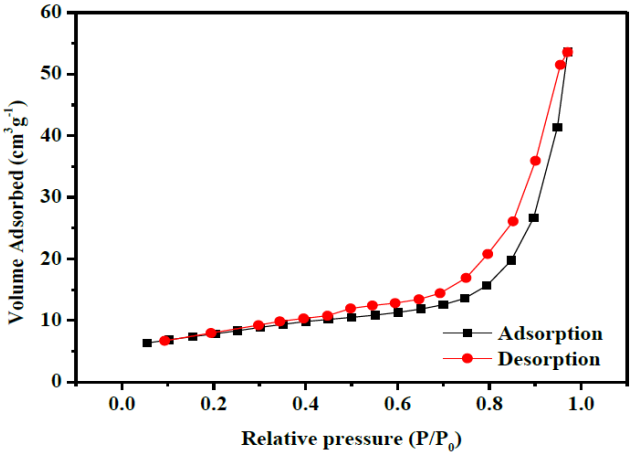

Figure 3. N2 adsorption-desorption isotherms of Ca0.5Mg0.5Co2O4 nanosheets.

It is reported that effect of NaOH may play an crucial role in determining the activity of nanocatalysts in AB hydrolysis, So, the catalytic behaviors of the $Ca_{0.5}Mg_{0.5}Co_2O_4$nanosheets are investigated in the presence of different NaOH dosage in the reaction system and the results are shown in Figure 4.

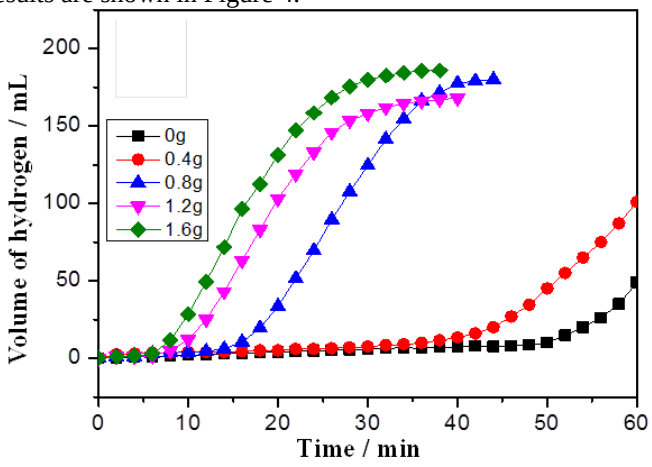

Figure 4. Hydrogen evolution from AB solution in the presence of different NaOH dosage.

As can be seen, when no NaOH is added in the reaction solution, nearly no hydrogen is produced at reaction time of 50 min and only 35 mL hydrogen is generated at reaction time of 60 min. In contrast, the hydrogen production rate is significantly improved in the presence of NaOH. Increase of NaOH dosage in the reaction solution will result in the increase of hydrogen generation rate. At NaOH dosage of 1.6 g, about 175 mL hydrogen is obtained at reaction time of 25 min. The corresponding turnover frequency (TOF) is about 4.8 $mol_{hydrogen}$ min^{-1} mol_{cat}^{-1}. According to the reaction formula of AB hydrolysis, $H_3NBH_3(aq) + 2H_2O(l) \rightarrow NH_4^+(aq) + BO_2^-(aq) + 3H_2(g)$, NH_4^+ ions will be formed as the hydrolysis reaction proceeds, which will be consumed by OH^- by the following route. $NH_4^+ + OH^- \rightarrow NH_3 + H_2O$. So, the rate of hydrolytic reaction was enhanced when OH^- is in the reaction system [19]. It should be mentioned that the activity of our catalyst is higher than that that of many noble-metal-free catalysts, such as Cu/RGO (TOF=3.61 $mol_{hydrogen}$ min^{-1} mol_{cat}^{-1}) [20], Cu/SiO_2 (TOF=3.24 $mol_{hydrogen}$ min^{-1} mol_{cat}^{-1}) [21], Co/Ti (TOF=1.7 $mol_{hydrogen}$ min^{-1} mol_{cat}^{-1}) [22], Ni/BN sheet (0.092) (TOF=1.24 $mol_{hydrogen}$ min^{-1} mol_{cat}^{-1}) [23].

Figure 5 shows that the hydrogen evolution when different amount of catalysts is used. As shown, the hydrogen production rate will increase as the increase of catalyst dosage. At reaction time of 20 min, 18 mL, 28 mL, 30 mL, 107 mL and 168 mL hydrogen will be generated when the catalyst dosage is 2.5 mg, 5.0 mg, 7.5 mg, 10.0 mg and 125.mg, respectively. Note that the hydrogen generation rate is slow at the early stage of the hydrolytic reaction, but increases remarkably at the middle state of the reaction. According to the literature, the oxides of transition metal themselves are inactive to AB hydrolysis [24]. However, AB in the hydrolysis system can also act as a reducing agent with mild reducibility and reduce oxides of Co to metallic Co on the catalyst surface, which exhibits high catalytic activity in AB hydrolysis. Due to the low reduction electrode potentials of Co^{2+}/Co (-0.28 V *vs.* SHE), it will take a relative long time for AB to reduce the oxide of Co to metallic state.[24] Thus, a relatively long induction time is necessary for initialized the hydrolysis reaction. It should be noticed that the induction time will decrease as the increase of catalyst dosage.

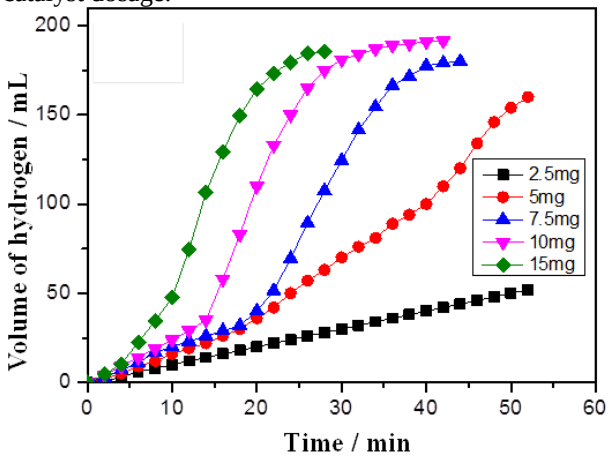

Figure 5. Hydrogen evolution at different catalyst dosage.

To study the effect of reaction temperature on the hydrogen evolution from AB solution, hydrolytic reaction was carried out in the temperature range from 25 to 45 ^oC. Figure 5 is the temperature-dependent hydrogen evolution

curves when the $Ca_{0.5}Mg_{0.5}Co_2O_4$ nanosheets act as catalysts. It is found that the hydrogen production rate will increase when the hydrolysis temperature is elevated. For example, at reaction temperature of 25 ^oC, nearly no hydrogen is released at reaction time of 10 min. In contrast, when the reaction temperature increases to 45 ^oC, about 190 mL hydrogen is obtained at reaction time of 10 min. This observation is in agreement with many results reported in the literature that rising the temperature is favorable for hydrogen release from AB solution [21, 25].

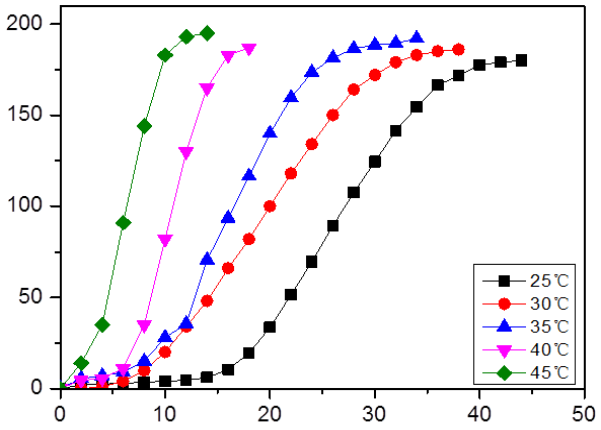

Figure 6. Hydrogen evolution at different reaction temperatures.

IV. CONCLUSIONS

In summary, we have prepared a novel catalyst for the AB hydrolysis, $Ca_{0.5}Mg_{0.5}Co_2O_4$ nanosheets composed of nanoparticles. In the hydrolytic reaction, the hydrogen production rate will increase as the increase the NaOH dosage. At NaOH dosage of 1.6 g, the turnover frequency is 4.8 $mol_{hydrogen}$ min^{-1} mol_{cat}^{-1}. It is also found that a high catalyst dosage and a high reaction temperature are favorable for the fast hydrogen release from ammonia solution. Considering its high catalytic activity and low cost, the $Ca_{0.5}Mg_{0.5}Co_2O_4$ nanosheet catalyst may find important applications in the catalytic AB hydrolysis for hydrogen production.

ACKNOWLEDGMENT

This work was financially supported by the Natural Science Foundation of Guangdong Province (No. 2016A030313120), the Excellent Youth Foundation of the University in Guangdong Province (No. YQ2015154), Natural Science Foundation of Huizhou University (No. 20160226013501332).

REFERENCES

[1] J. Baxter, Z.X. Bian, G. Chen, D. Danielson, M.S. Dresselhaus, A.G. Fedorov, T.S. Fisher, C.W. Jones, E. Maginn, U. Kortshagen, A. Manthiram, A. Nozik, D.R. Rolison, T. Sands, L. Shi, D. Sholl, Y.Y. Wu, Energy Environ. Sci. 2 (2009) 559.

[2] A. Sartbaeva, V.L. Kuznetsov, S.A. Wells, P.P. Edwards, Energy Environ. Sci. 1 (2008) 79.

[3] T.S. Uyar, D. Besikci, Int. J. Hydrogen Energy 42 (2017) 2453.

[4] Q.-L. Zhu, Q. Xu, Energy Environ. Sci. 8 (2015) 478.

[5] M. Yadav, Q. Xu, Energy Environ. Sci. 5 (2012) 9698.

[6] U.B. Demirci, Int. J. Hydrogen Energy 42 (2017) 9978.

[7] T. Sadhasivam, H.-T. Kim, S. Jung, S.-H. Roh, J.-H. Park, H.-Y. Jung, Renew. Sust. Energy Rev. 72 (2017) 523.

[8] U.B. Demirci, P. Miele, Energy Environ. Sci. 2 (2009) 627.

[9] U.S. Department of Energy, Office of Energy Efficiency and Renewable Energy. Technical System Targets: Onboard Hydrogen Storage Systems for Light-Duty Vehicles; Available at the following: http://energy.gov/sites/prod/files/2015/01/f19/fcto_myrdd_table_onboard_h2_storage_systems_doe_targets_ldv.pdf.

[10] Q. Xu, M. Chandra, J. Power Sources 163 (2006) 364.

[11] J. Manna, S. Akbayrak, S. Özkar, Appl. Catal. B 208 (2017) 104.

[12] M.A. Khalily, H. Eren, S. Akbayrak, H.H. Susapto, N. Biyikli, S. Özkar, M.O. Guler, Angew. Chem. Int. Ed. 55 (2016) 12445.

[13] P.-H. Liu, M. Wen, C.-S. Tan, M. Navlani-Garc á, Y. Kuwahara, K. Mori, H. Yamashita, L.-J. Chen, Nano Energy 31 (2017) 57.

[14] J.-X. Kang, T.-W. Chen, D.-F. Zhang, L. Guo, Nano Energy 23 (2016) 145.

[15] L.B. Wang, H.L. Li, W.B. Zhang, X. Zhao, J.X. Qiu, A.W. Li, X.S. Zheng, Z.P. Hu, R. Si, J. Zeng, Angew. Chem. Int. Ed. 56 (2017) 4712.

[16] Ö. Metin, M. Dinc, Z.S. Eren, S. Özkar, Int. J. Hydrogen Energy 36 (2011) 11528.

[17] J.-M. Yan, X.-B. Zhang, H.S. Shioyama, Q. Xu, J. Power Sources 195 (2010) 1091.

[18] S. Karahan, S. Özkar, Int. J. Hydrogen Energy 40 (2015) 2255.

[19] J. Yan, J. Liao, H. Li, H. Wang, R. Wang, Catal. Commun. 84(2016)124.

[20] Y.W. Yang, Z.-H. Lu, Y.J. Hu, Z.J. Zhang, W.M. Shi, X.S. Chen, T.T. Wang, RSC Adv. 4 (2014) 13749.

[21] Q.L. Yao, Z.-H. Lu, Z.J. Zhang, X.S. Chen, Y.Q. Lan, Sci. Rep. 4 (2014) 7597.

[22] J. Liao, H. Li, X. Zhang, Catal. Commun. 67 (2015) 1.

[23] X.J. Yang, L.L. Li, W.L. Sang, J.L. Zhao, X.X. Wang, C. Yu, X.H. Zhang, C.C. Tang, J. Alloy. Compd. 693 (2017) 642.

[24] V.I. Simagina, O.V. Komova, A.M. Ozerova, O.V. Netskina, G.V. Odegova, D.G. Kellerman, O.A. Bulavchenko, A.V. Ishchenko, Appl. Catal. A 394 (2011) 86.

[25] J.Y. Liao, H. Li, X.B. Zhang, K.J. Feng, Y.L. Yao, Catal. Sci. Technol. 6 (2016) 3893.